# MODELING OF NONLINEAR FERROMAGNETIC CORES

LUCIAN MANDACHE[1], DUMITRU TOPAN [2], KAMAL AL-HADDAD[3]

**Key words: Ferromagnetic core, Eddy current losses, Modeling, Time-domain simulation, SPICE subcircuit.**

The paper presents an advanced modeling technique of ferromagnetic cores, entirely based on Maxwell's theory. Our models answer to common modern applications of electrical engineering. They use nonlinear electrical equivalent diagrams, easy to built according to the core geometry (including air-gaps) and ferromagnetic material characteristics. The core model is compatible to be included in the entire circuit model, being suitable for the time-domain analysis. The circuit analysis provides complete information on any working parameters of the magnetic core (as the main and leakage time-domain magnetic fluxes, position and shape of minor magnetizing loops, instantaneous and mean eddy current losses, dynamic permeabilities, dynamic inductances, etc.), as well as of other parts of the analyzed circuit.

## 1. **INTRODUCTION**

Circuit parts with ferromagnetic cores (as electric transformers, electromagnets, reactance or filtering coils, etc.) are capital components for a wide range of engineering applications. Their rigorous modeling, considering the magnetic saturation phenomena, the hysteresis and eddy currents, allows an optimal design of such devices, as well as an accurate analysis of steady state or transient regimes of any circuit including such nonlinear devices [1].

Many models for nonlinear ferromagnetic cores have been proposed. They are generally fully analytic models based on certain physical theories like Weiss, Preisach or Jiles-Atherton, often restricted to particular applications [2–4]. Some apparently accurate models are inadequate when used in circuit simulation because of discontinuities which can provoke severe convergence problems and therefore, alter the simulation results. For many known models used in circuit simulators [5–7], it is difficult to identify the correct correspondence between the model parameters and the real device ones.

[1] University of Craiova, Faculty of Electrical Engineering, Decebal Blv. 107, Craiova 200440, Romania; lmandache@elth.ucv.ro

[2] University of Craiova, Faculty of Electrical Engineering, dtopan@central.ucv.ro

[3] École de Technologie Supérieure de Montréal, 1100 rue Notre-Dame Ouest, Montréal (Québec) Canada, H3C 1K3; kamal@ele.etsmtl.ca

Rev. Roum. Sci. Techn. – Électrotechn. et Énerg., **53**, *4*, p. 403–412, Bucarest, 2008

The paper use a modeling approach based on electric circuit analogy [1,5–7]. One conceives equivalent nonlinear lumped circuits according to the core geometry (including air-gaps and leakage paths) and ferromagnetic material characteristics. The whole circuit (including the core) analysis provides complete information on all working parameters of the magnetic core (as the main and leakage time-domain magnetic fluxes, position and shape of minor magnetizing loops, instantaneous and mean eddy current losses, dynamic permeabilities, dynamic inductances, etc.), as well as of other parts of the analyzed circuit [8, 9].

## 2. **MODELING OF A FERROMAGNETIC PIECE**

The Fig. 1 suggests the modeling of a homogenous magnetic circuit branch, through an electric voltage controlled nonlinear resistance. The nonlinear function is formally the same [1] for following relationships:

– $\varphi = f(u_m)$, the fascicular magnetic flux vs. the magnetic force across the ferromagnetic piece;

– $i = f(u)$, the current vs. the voltage across the nonlinear resistance.

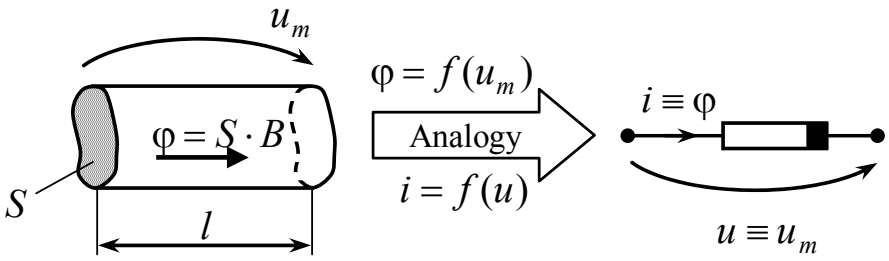


Fig. 1 – Modeling of a ferromagnetic piece, with ignoring eddy currents.

The rigorous study of transient and steady state harmonic or distorted regimes requires to complete the simple model of Fig. 1, in order to consider the eddy currents, their losses and their own magnetic field. One considers a homogenous piece of ferromagnetic core, crossed by an uniform magnetic field on the cross section (Fig. 2). The induced electromotive force along the closed loop $\Gamma$, drawn as an eddy current line, is given by the Faraday's law

$$e_\Gamma(t) = -S_\Gamma\left(\frac{\mathrm{d}B}{\mathrm{d}t}\right), \tag{1}$$

and the elementary eddy current, nearby the loop $\Gamma$ is

$$\mathrm{d}i_e = S_\Gamma\left(\frac{\mathrm{d}B}{\mathrm{d}t}\right)\cdot\frac{l\sin\alpha}{\rho l_\Gamma}\mathrm{d}r\,, \tag{2}$$

where $\rho$ is the material resistivity and $l$ the length of the piece. If the point O is located where the eddy current density is equal to zero, the total eddy current becomes

$$i_e(t) = K_1\frac{l}{\rho}\left(\frac{\mathrm{d}B}{\mathrm{d}t}\right), \tag{3}$$

where

$$K_1 = \int_0^{r_0}\frac{S_\Gamma\sin\alpha}{l_\Gamma}\cdot\mathrm{d}r\,. \tag{4}$$

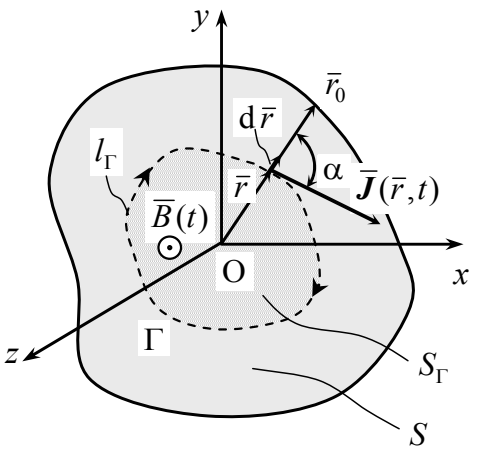


Fig. 2 – Cross section of a ferromagnetic piece.

If $\varphi$ is the magnetic flux through the considered ferromagnetic piece, then

$$i_e(t) = K\cdot\left(\frac{\mathrm{d}\varphi}{\mathrm{d}t}\right), \tag{5}$$

from where

$$K = K_1\cdot\frac{l}{\rho}\cdot\frac{1}{S}. \tag{6}$$

The instantaneous losses due to the computed eddy current are

$$p(t) = K_2 \frac{l}{\rho}\left(\frac{\mathrm{d}B}{\mathrm{d}t}\right)^2, \tag{7}$$

where

$$K_2 = \int_0^{r_0} \frac{S_\Gamma^2 \sin\alpha}{l_\Gamma} \cdot \mathrm{d}r\,. \tag{8}$$

One defines the equivalent resistance

$$R_e = \frac{p(t)}{i_e^2}, \tag{9}$$

associated to the current $i_e$ and the losses $p$. One results

$$R_e = \frac{K_2}{K_1^2} \cdot \frac{\rho}{l}\,. \tag{10}$$

Considering the quantities $i_e$, $K$, $R_e$ given above, the simple model of Fig. 1 requires new elements, according to the equivalent diagram of Fig. 3, that includes the eddy current losses phenomena.

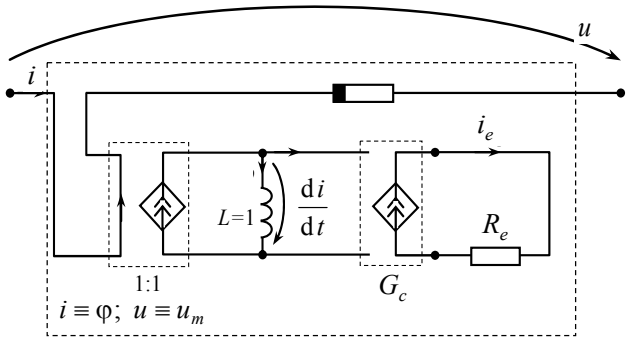


Fig. 3 – Modeling of a ferromagnetic piece, considering eddy current losses.

In this model, the flux derivative is obtained as the voltage across the ideal unity inductance crossed by a current numerically equal to the magnetic flux, injected through a unity gain current controlled current source. The equivalent eddy

current is given by a voltage controlled current source with the transfer conductance $G_c$ numerically equal to the constant $K$, according to eq. (5).

Concrete expressions of the form factors $K_1$, $K_2$, as well as the quantities $G_c$, $i_e$, $p$, $R_e$ are given in the table 1 for some convenient cases.

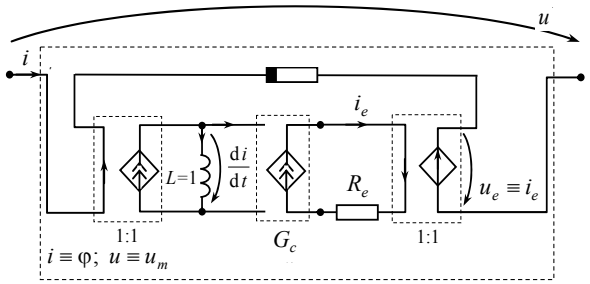


Fig. 4 – Modeling of a ferromagnetic piece, considering eddy current losses and their parasitic magnetic field.

*Table 1*

Model parameters for some convenient cross sections of ferromagnetic pieces

| Model parameter | 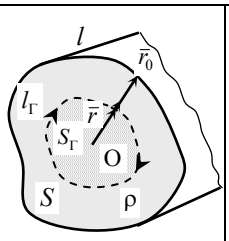 | 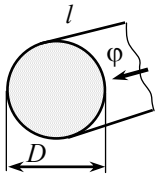 | 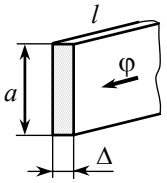 | 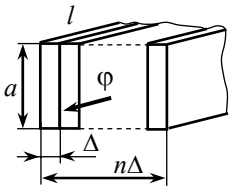 |
|---|---|---|---|---|
| | Irregular cross section | Cylinder | Ferromagnetic steel sheet | Steel sheet core ($n$ sheets) |
| $K_1$ | $K_1 = \int_0^{r_0} \frac{S_\Gamma \sin\alpha}{l_\Gamma} \cdot \mathrm{d}r$ | $K_1 = \frac{D^2}{16}$ | $K_1 = \frac{\Delta^2}{8}$ | $K_1 = n\frac{\Delta^2}{8}$ |
| $K_2$ | $K_2 = \int_0^{r_0} \frac{S_\Gamma^2 \sin\alpha}{l_\Gamma} \cdot \mathrm{d}r$ | $K_2 = \frac{\pi D^4}{128}$ | $K_2 = \frac{a\Delta^3}{12}$ | $K_2 = n\frac{a\Delta^3}{12}$ |
| $i_e$ | $i_e(t) = K_1 \frac{l}{\rho}\left(\frac{\mathrm{d}B}{\mathrm{d}t}\right)$ | $i_e(t) = \frac{D^2 l}{16\rho}\left(\frac{\mathrm{d}B}{\mathrm{d}t}\right)$ | $i_e(t) = \frac{\Delta^2 l}{8\rho}\left(\frac{\mathrm{d}B}{\mathrm{d}t}\right)$ | $i_e(t) = n\frac{\Delta^2 l}{8\rho}\left(\frac{\mathrm{d}B}{\mathrm{d}t}\right)$ |
| $G_c$ | $G_c = K_1 \cdot \frac{l}{\rho} \cdot \frac{1}{S}$ | $G_c = \frac{l}{\rho} \cdot \frac{1}{4\pi}$ | $G_c = \frac{l}{\rho} \cdot \frac{\Delta}{8a}$ | $G_c = \frac{l}{\rho} \cdot \frac{\Delta}{8a}$ |

| | | | | |
|---|---|---|---|---|
| $p$ | $p(t) = K_2 \frac{l}{\rho}\left(\frac{\mathrm{d}B}{\mathrm{d}t}\right)^2$ | $p(t) = \frac{\pi D^4 l}{128\rho}\left(\frac{\mathrm{d}B}{\mathrm{d}t}\right)^2$ | $p(t) = \frac{a\Delta^3 l}{12\rho}\left(\frac{\mathrm{d}B}{\mathrm{d}t}\right)^2$ | $p(t) = n\frac{a\Delta^3 l}{12\rho}\left(\frac{\mathrm{d}B}{\mathrm{d}t}\right)^2$ |
| $R_e$ | $R_e = \frac{K_2}{K_1^2}\cdot\frac{\rho}{l}$ | $R_e = \frac{\rho}{l}\cdot 2\pi$ | $R_e = \frac{\rho}{l}\cdot\frac{16a}{3\Delta}$ | $R_e = \frac{1}{n}\cdot\frac{\rho}{l}\cdot\frac{16a}{3\Delta}$ |

Although the model above considers the core losses, it is not yet complete because it does not consider the parasitic magnetic field produced by the eddy currents. The magnetic force produced by the equivalent eddy current is given by a unity gain current controlled voltage source, according to the Ampere's law, as in Fig. 4.

Therefore, we obtained a proper model for transients and strongly distorted regimes, as in modern electrical engineering applications.

## 3. **MODEL IMPLEMENTATION**

In order to implement the model above, one needs the electric resistivity of the ferromagnetic material. Since this parameter is not usually available in the manufacturer's datasheet, one may using the specific power losses in order to find the model parameters. The specific power losses included in the datasheet $p_0$ [W/kg] are given for a certain frequency $f_0$ (state harmonic regime) and a certain peak value of the magnetic flux density $B_0$. It results the average value of power losses for these operating conditions, corresponding to the considered ferromagnetic piece

$$P_0 = p_0 \gamma S l\,, \tag{11}$$

where $\gamma$ is the density of the ferromagnetic material.

One computes the mean power losses, in the same conditions, starting from eq. (7)

$$P_0 = K_2 \cdot \frac{l}{\rho}\cdot \int_0^{1/f_0}\left(\frac{\mathrm{d}}{\mathrm{d}t}B_0 \sin 2\pi f_0 t\right)^2 \mathrm{d}t\,, \tag{12}$$

from where

$$P_0 = K_2 \cdot \frac{l}{\rho}\cdot 2\pi^2 f_0^2 B_0^2\,. \tag{13}$$

The expressions (11) and (13) guide us to the resistivity

$$\rho = K_2 \cdot \frac{2\pi^2 f_0^2 B_0^2}{p_0 \gamma S}, \tag{14}$$

the control conductance

$$G_c = \frac{K_1}{K_2} \cdot \frac{p_0 \gamma l}{2\pi^2 f_0^2 B_0^2}, \tag{15}$$

and the equivalent resistance

$$R_e = \left(\frac{K_2}{K_1}\right)^2 \cdot \frac{2\pi^2 f_0^2 B_0^2}{p_0 \gamma l S}. \tag{16}$$

For the convenient applications, one obtains:

– circular cylinder (diameter $D$): $G_c = \dfrac{4 p_0 \gamma l}{\pi^3 D^2 f_0^2 B_0^2}$, $R_e = \dfrac{\pi^3 D^2 f_0^2 B_0^2}{8 p_0 \gamma l}$,

– steel sheet pack: $G_c = \dfrac{3 p_0 \gamma l}{4\pi^2 a \Delta f_0^2 B_0^2}$, $R_e = \dfrac{8\pi^2 \Delta f_0^2 B_0^2}{9 p_0 \gamma l}$.

As useful implementation of the above described model, we performed a SPICE subcircuit (shown in Appendix) which can be included in any time-domain circuit simulation.

The subcircuit body contains the parameters bound to ferromagnetic material properties, usually included in datasheets – $B_0, f_0, p_0, \gamma$, as well as the nonlinear first magnetization characteristic *B–H* given by points. Subcircuit calls contain geometric parameters only – the cross-section, the length of the core piece and a constant factor which depends on the above defined form factors; they will be passed to the subcircuit beside the material parameters. The magnetic reluctances of air gaps and leakage paths are modeled by linear resistances.

## 4. **EXAMPLES**

As first example, using the model of Fig. 4, one builds the lossy nonlinear characteristic of a ferromagnetic piece having the length of 100 mm and the cross section of 10 $\text{cm}^2$, the specific losses of 2 W/kg at 50 Hz and 1 T. The magnetization cycle has been simulated and depicted for 50 Hz (Fig. 5a), respectively 400 Hz (Fig. 5b), the obtained results being proven experimentally.

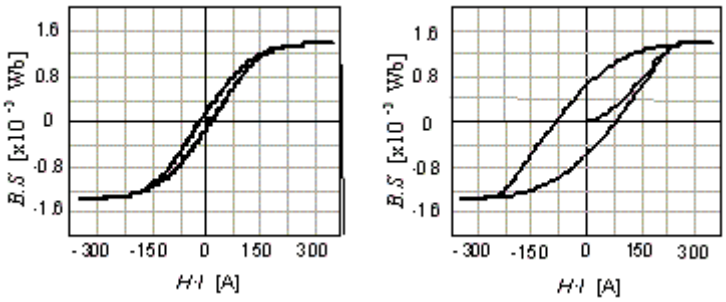


a b

Fig. 5 – Example of a lossy nonlinear characteristic modeled to: a) 50 Hz; b) 400 Hz.

As second example, one presents the simple case of an inductor used as series filter reactor for a rectified current (Fig. 6). The modeling circuit includes the equivalent circuit of the ferromagnetic core (including air gaps and leakage paths), as well as the two series connected windings, beside the network and the load.

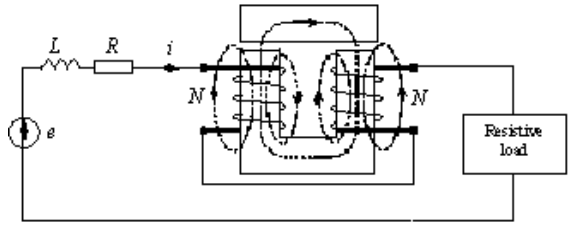


Fig. 6 – Series filter reactor.

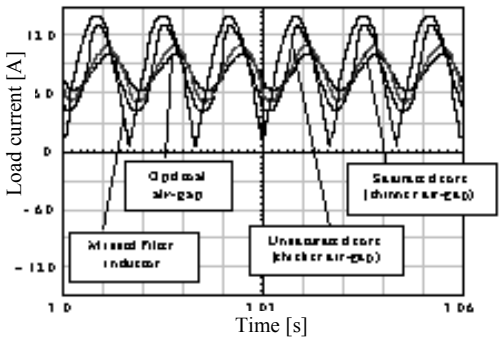


Fig. 7 – Smoothed load current for three values of the air-gap.

One searches for the optimal value of the adjustable air-gap in order to obtain the best smoothing effect. Three distinct results are shown, for three distinct values of the air gap. Fig. 7 shows the load current and Fig. 8 shows the corresponding magnetization cycles. Therefore, the optimal solution can be chosen without a doubt. For comparison, the Fig. 7 shows the load current when the inductor is missing.

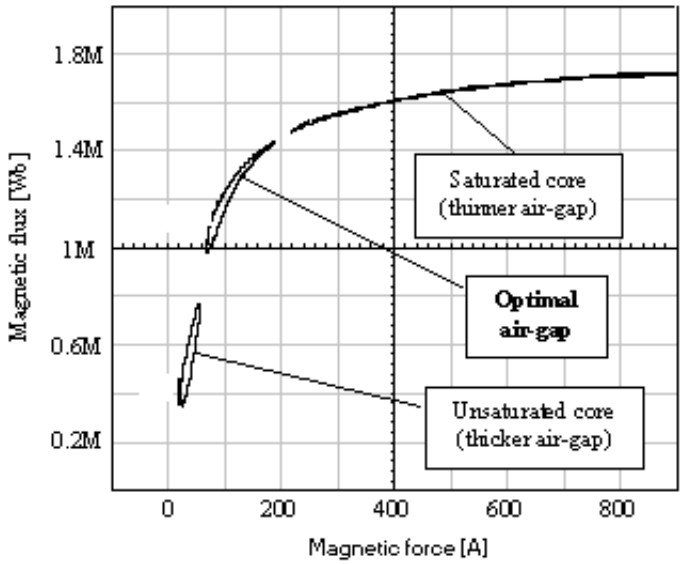


Fig. 8 – Magnetization cycles of the inductor core for three different values of the air-gap.

## 5. **CONCLUSIONS**

The optimal design of ferromagnetic devices aims minimal sizes and manufacturing costs. In order to attend the mentioned purposes, it requires a rigourous control of bias points, saturation level, core and copper losses, assuring at the same time all operating parameters of the whole equipment. In comparison to the previous approaches, the analytic approximations (often based on empiric considerations) are avoided and the model feasibility is developed in order to include it in common time-domain analysis programs, like SPICE. The developed model is suitable from low to medium working frequencies, including switching regimes, as in power electronics applications. Some experimental results, performed for some particular cases, confirm the accuracy and reliability of the proposed model. Therefore, the paper may be a really useful tool for researchers and designers.

## APPENDIX

### SPICE subcircuit as time-domain model of a ferromagnetic piece. Example.

```
.SUBCKT RELUC  1 4 {B0=1.0  F0=50  P0=1.3  GAMMA=7650}
V1 1 2
B1 2 3  I= V(9)*{SFE}
E1 8 0 2 3 {1/LFE}
A1 8 9 BH_FCT
.MODEL BH_FCT  PWL(XY_ARRAY= [-15.0K, -1.73;  -10.0K, -1.71;
+ -7.0K, -1.664; -6.0K, -1.638; -5.0K, -1.602; -4.0K, -1.56; -3.5K, -1.535;
+ -3.0K, -1.5; -2.5K, -1.45; -2.0K, -1.38; -1.8K, -1.34; -1.6K, -1.3;
+ -1.4K, -1.24; -1.2K, -1.17; -1.0K, -1.06; -900.0, -1.0; 900.0, 1.0;
+ 1.0K, 1.06; 1.2K, 1.17; 1.4K, 1.24; 1.6K, 1.3; 1.8K, 1.34;
+ 2.0K, 1.38; 2.5K, 1.45; 3.0K, 1.5; 3.5K, 1.535; 4.0K, 1.56;
+ 5.0K, 1.602; 6.0K, 1.638; 7.0K, 1.664; 10.0K, 1.71;
+ 15.0K, 1.73] INPUT_DOMAIN=100M FRACTION=TRUE)
F1 0 7 V1 1
L1 7 0 1H
G1 6 0 7 0  {1/K*GAMMA*P0*LFE/(2*SFE*B0^2*F0^2)}
B2 0 5 V=I(V2)*{(K*B0^2*F0^2*SFE)/(GAMMA*P0*LFE)}
V2 5 6
H1 3 4 V2 1
.ENDS
```

*Received on 17 February, 2008*

## REFERENCES

1. L. Mandache, K. Al-Haddad, *High Precision Modeling of Nonlinear Lossy Magnetic Devices*, IEEE International Symposium of Power Electronics – ISIE 2006, 9–13 July 2006, Montreal, pp. 267–2676.
2. D. C. Jiles, D.L. Atherton, *Ferromagnetic Hysteresis*, IEEE Transactions on Magnetics, **Mag-19**, *5*, pp. 2183–2185 (1983).
3. F. Fiorillo, L. R. Dupré, *Comprehensive Model of Magnetization Curve, Hysteresis Loops, and Losses in Any Direction in Grain-Oriented Fe-Si*, IEEE Transactions on Magnetics, **38**, *3*, pp. 1467–1476 (2002).
4. D. Carnevale, S. Nicosia, L. Zaccarian, *Generalized Constructive Model of Hysteresis*, IEEE Transactions on Magnetics, **42**, *12*, pp. 3809–3817 (2006).
5. H. G. Brachtendorf, C. Eck, R. Laur, *Macromodeling of Hysteresis Phenomena with SPICE*, IEEE Transactions on Circuits and Systems – II: Analog and Digital Signal Processing, **44**, *5*, pp. 378–388 (1997).
6. J. H. Chan, A. Vladimirescu, X. C. Gao, P. Liebmann, J. Valainis, *Nonlinear Transformer Model for Circuit Simulation*, IEEE Transactions on Computer-Aided Design, **10**, *4*, pp. 476–482 (1991).
7. M. O'Hara, *Modeling Non-Ideal Inductors in SPICE*, www.intusoft.com.
8. M. Iordache, L. Mandache, M. Perpelea, *Analyse numérique des circuits analogiques non linéaires*, Ed. Groupe Horizon, Marseille, 2006.
9. D. Topan, L. Mandache, *Chestiuni speciale de analiza circuitelor electrice*, Edit. Universitaria, Craiova, 2007.